Journal of Bio & Geo Material and Energy (BiGME)
Volume 5 No. 1, March 2025
P-ISSN: 2808-1560 E-ISSN: 2808-1404

Photodegradation of some Antibiotics and Industrial Dye by Visible Light of Highly Active Synthesized PAni/TiO_2 Nanocomposite Photocatalyst

A.A. Mahmoud[1], S.B. Ali[2], D.A. Ajiya[1], M. Muhammad[1]
[1]Department of Chemistry, Faculty of science, Abubakar Tafawa Balewa University, Bauchi P.M.B. 0248 Bauchi, Bauchi State
[2,]Nigerian Army University Biu Nigeria

Email: aamahmoud@atbu.edu,ng

Article info:

Submitted: January 2025
Revised: February 2025
Accepted: February 2025
Published: March 2025

Abstract:
The presence of pharmaceuticals and dyes in the environment poses significant threats to human health and ecosystems. This study develops a novel Polyaniline/Titanium Dioxide (PAni/TiO_2) nanocomposite photocatalyst for the efficient photodegradation of tetracycline and methylene blue. Characterization techniques, including FTIR, FESEM, EDX, DRS, and TGA, confirmed the successful formation of the nanocomposite. Under UV and visible light irradiation, The optimal condition for maximum tetracycline and methylene blue degradation efficiency was obtained to be 92% and 95%, respectively, with 100 mg of PAni/TiO_2 nanocomposite, 100 ml of Tetracycline, and pH 7.0 after 120 min of exposure to UV and visible light. Optimum reaction conditions, including catalyst concentration, initial dye concentration, and reaction time, were investigated. This research demonstrates the potential of PAni/TiO_2 nanocomposite as a promising photocatalyst for the degradation of organic pollutants

Keywords: Polyaniline/Titanium Dioxide **(**PAni/TiO_2) Nanocomposite, Photodegradation, Photocatalyst, Antibiotics, Dyes, Organic pollutants

1. Introduction

Nanotechnology has emerged as a pivotal area of research in material sciences, with the synthesis of nanoparticles (NPs) gaining significant attention globally. Notably, NPs exhibit unique properties due to their large surface area-to-size ratio, enabling enhanced interactions with other molecules (Khawla, 2020). Nanostructures formed by conducting polymers showed properties differing from their bulk structures, such as increased conductivity of nanotubes with respect to the conventional conducting polymer (Adamu et al., 2015,Martin-Yerga, Gonzalez-Garcia, & Costa-Garcia, 2014), and increased charge transport rates compared to conventional conducting polymers (Dhand et al., 2011; Mahmoud et al., 2020). The good conductivity and increased surface area of conducting polymers couple with its highly conjugated length (Mahmoud et al., 2022) make them suitable candidates for electrochemical application including electronics, photonics, mechanics and sensing (Lu et al., 2006).

The ability of PAni to combined with different nanoparticles to form the nanocomposite has great potential applications such as radar-absorber (Makeiff & Huber, 2006), indicators (Drelinkiewicz et al., 2007), electrochemical and capacitors (Sun & Deng, 2008), Bioelectronic components (Mahmoud et al., 2022), catalysts (Mahmoud et al., 2024) and gas separation membrane (Weng et al., 2011).

NPs can be categorized into inorganic (semiconductor, metallic, and magnetic) and organic (carbon-based) types. Surface-modified NPs are designed for specific applications, leveraging their catalytic activity, optical properties, and mechanical strengths (Mounika and Manogna, 2017). Conducting polymers like polyaniline (PAni) have been used to enhance TiO_2 photocatalytic efficiency due to their charge carrier mobility and visible-light absorption (Diksha and Ruby, 2021). Titanium dioxide (TiO_2) is a valuable material in various fields, boasting unique surface chemistry, high chemical stability, and non-toxicity. However, existing synthesis methods for PAni/TiO_2 nanocomposites often involve hazardous chemicals,

prompting the need for eco-friendly, cost-effective approaches. This study aims to synthesize, characterize, and explore the photocatalytic application of PAni/TiO_2 nanocomposite.

2. Research Methods

Chemicals and Reagents

All chemical and reagents used are of analytical grade and were used without further purification. Ammonium peroxydisulfate (APS) will be used to initiate the polymerisation, Phosphoric acid (H_3PO_4) was used as doping agent, Acetonitrile, CH_2Cl_2, Formic acid, Aniline, HCl, $(NH_4)_2S_2O_8$, Deionized water, H_2O_2, titanium tetra isopropoxide (TTIP), ethanol, Methylene blue, Tetracycline and Levofloxacin.

Instruments and Equipment

N_2 adsorption-desorption for surface area and pore size analysis using Brunauer-Emmett-Teller (BET) method, Ultrasonic Machine, Magnetic stirrer, X-ray diffraction (XRD), scanning electron microscopy, diffuse reflectance spectroscopy (DRS), energy dispersive X-ray (EDX), thermogravimetric analysis (TGA), fourier transform infrared (FTIR) spectroscopy, atomic force microscopy (AFM) and universal Attenuated total reflectance (ATR) are commonly used.

Research Procedures

Synthesis of Polyaniline

A 4.5 ml aniline was injected into 70 ml of 2 M HCl and was sonicated for 30 min. After 1/2 h, 11.5 g (NH4)2S2O8 was dropped into the solution with constant stirring. The polymerization was allowed to proceed for 2 h at 25 oC. The Reaction mixture was filtered under gravity, and was washed with 2.0 M HCl and de-ionized water, After wards it was dried at 60 oC for 24 h under vacuum to obtain a fine tint green powder (Nasirian and Moghaddam, 2014; Fleaca, et al., 2016).

Synthesis of Titanium Dioxide

TiO_2 nanoparticles was prepared using H_2O_2 solution added to 10 ml of 1 mol L^{-1} ethanol solution of titanium tetra isopropoxide (TTIP). Ethanol was added to the brown colored solution and the total volume of the solution was adjusted to 100 ml. The solution was then heated at 60 ^oC for 1 h in a closed vessel. The solution was calcined at 600 ^oC for 3 h and a white titanium oxide powder was obtained (Choudhury et al., 2013; Lee et al., 2015; Jongprateep et al., 2015).

Synthesis of PAni/TiO_2

Nanocomposite of /PAni/TiO_2 Synthesis was prepared after 5 µL (0.06 mmol) aniline injected to 7.5 ml phosphate buffer pH 4.3 containing nano-TiO_2 with constant stirring for 15 min at room temperature. To reduce aggregation of TiO_2 nanoparticles, ultrasonic action was needed for 30 min. Then 0.0009 g (0.004 mmol) SPS (based on molecular repeat unit) was added to the solution and stirred for 30 min, afterward 0.5 APS was be added to the solution. Polymerization was start after 60 min, 2.25 ml (0.02 M) H_2O_2 was added drop-wise with constant stirring and After 24 h, the reaction mixture was filtered with sinter-glass and dried in vacuum oven at 60^oC for 24 h and a fine tint green powder was obtained (Arora et al., 2015; Wang et al., 2013).

Photocatalytic degradation experiments

Photocatalytic degradation experiments were performed at various parameters such as concentration of dye, pH of solution, time of UV light illumination, and dose of photocatalyst. The variation of absorbance of dye solution at various parameters in the presence of TiO2/PAni nanocomposite was recorded. Photocatalytic degradation % efficiencies (η) was obtained using following equation.

$$\% \eta = VBo - VBF / VBo \times 100$$

where VBo is the initial absorbance and VBF is the final sampled absorbance (Azad et al., 2018)

Photodegradation of dye (Methylene blue)

The dye was used as a model pollutant for photodegradation.100 mg of the nanocomposite in 250 ml beaker which contains 100 ml of the dye solution under ultrasonication for 20 min. Furthermore, the mixed solution was kept in a chamber at the dark condition to attain the absorption desorption equilibrium. The photodegradation of the dye was recorded with the help of UV–Visible irradiation at every 30 min regular interval from 0 to 120 min. The absorbance of the dye was recorded using 200 µl volume and 10 cm length quartz cuvette. Then the dye degradation efficiency was calculated (Aravin et al., 2021).

Photocatalytic degradation of the drugs (Tetracycline)

For the photo-degradation process, 50 mg synthesized photocatalyst was added in 100 ml of the drug solution (20 mg/L), stirring for 1 h in dark condition to achieve adsorption–desorption equilibrium. In this equilibrium state, 4 ml solution was taken and centrifuged to remove the sample from the suspension to analyze the concentration of the drug using a UV–vis spectrophotometer. After which the remaining solution was exposed to sunlight radiation under stirring at 800 rpm to degrade the drug solution. Every 10 min, 4 ml of light exposed solution was taken and centrifuged at maximum rpm to discrete the photocatalyst. Then the concentration of drug was determined using a UV–vis spectrophotometer. Finally, the rate of photo-degradation efficiency was evaluated by the below relation (Ahmad et al., 2020):

$$\text{Photo-degradation efficiency} = (C_0 - C_t / C_0) \times 100\ \%$$

Where, C_0 is the original concentration and C_t is the concentration after degradation at time t.

Characterization

Transmission Electron Microscopy (TEM) and Field Emission Scanning Electron Microscopy (FESEM) were used for surface morphology examination. Atomic Force Microscopy (AFM) for surface roughness and microstructure analysis in non-contact mode. Energy-Dispersive X-ray Spectroscopy (EDS) for elemental analysis

X-ray Photoelectron Spectroscopy (XPS) was use for chemical composition determination. X-ray Diffraction (XRD) Measurements (2θ range: 10° to 100°). Average crystallite size (τ) calculation using Scherer's formula

$\tau = \frac{0.9\lambda}{\beta cos\theta}$, Fourier transform infrared spectroscopy (FTIR) to carry out the molecular analysis of samples in the region of 400–4000 cm^{-1}, UV-Vis spectroscopy to determine absorbance spectra of the nanocomposites and electrodes, interferometer, nuclear magnetic resonance (NMR), Cyclic voltammetry, Attenuated total reflectance (ATR) sampling accessory. The pH measurements will be made with a pH meter

3. Results and Discussion

FTIR Analysis for Polyaniline (PAni) TiO_2 Nanoparticles and PAni/TiO_2 Nanocomposites

It can be seen from the figure1, that the FTIR spectrum of TiO_2 nanoparticles showed a prominent absorption band at 890 cm^{-1}, which is attributed to the Ti-O stretching vibration mode. This peak is a characteristic feature of TiO_2 nanoparticles, confirming their successful synthesis and the presence of Ti-O bonds.

The FTIR spectrum of PAni shows several distinct absorption bands at 3384 cm^{-1}, corresponding to N-H stretching vibrations, indicating the presence of amine groups, at 3056 cm^{-1}, corresponding to C-H in-plane bending vibrations, suggesting the presence of aromatic rings and at 1547 cm^{-1} and 1478 cm^{-1}, corresponding to C-N stretching of quinoid and benzenoid rings, respectively, which are characteristic of PAni's conductive structure. Additional peaks at 1297 cm^{-1}, 1114 cm^{-1}, and 797 cm^{-1} are attributed to various vibration bands and C-H stretching vibrations in the polymer backbone.

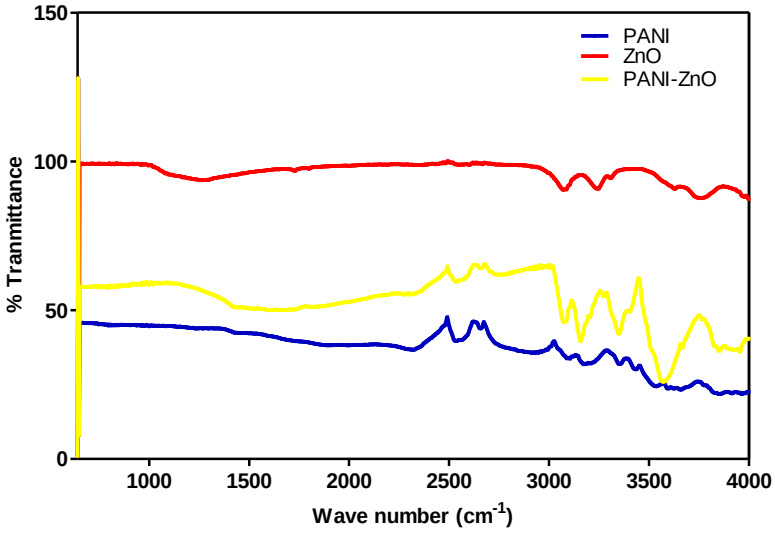

Figure 1. FTIR spectra of Polyaniline (PAni), TiO_2 nanoparticles and PAni/TiO_2 nanocomposite

The FTIR spectrum of PAni/TiO_2 nanocomposites exhibits a combination of absorption bands from both TiO_2 and PAni. The peak at 890 cm^{-1}, associated with Ti-O stretching, confirms the presence of TiO_2 within the composite. Peaks at 3384 cm^{-1}, 3056 cm^{-1}, 1547 cm^{-1}, 1478 cm^{-1}, and other positions correspond to the N-H, C-H, and C-N stretching vibrations from PAni, indicating the retention of PAni's functional groups within the composite.

New absorption bands or shifts in existing bands can also be observed, indicating possible interactions between TiO_2 and PAni, such as hydrogen bonding or coordination interactions.

The FTIR spectra reveal the successful incorporation of TiO_2 nanoparticles into the PAni matrix, forming a nanocomposite with distinct functional groups from both components. The retention of characteristic absorption bands from both TiO_2 and PAni suggests good compatibility and interaction at the molecular level.

The presence of new peaks or shifts in existing peaks in the PAni/TiO_2 spectrum indicates interactions between TiO_2 and PAni. These interactions are crucial for the enhanced properties of the nanocomposite, such as improved charge separation and enhanced photocatalytic activity.

The FTIR observations aligned well with recent studies on similar nanocomposites, a study by Sharma et al. (2020) Similarly, Zhang et al. (2021) highlighted the interactions between TiO_2 and PAni in the composite, indicated by shifts in the FTIR absorption bands.

The presence of functional groups and the interactions between TiO_2 and PAni in the nanocomposites are critical for their photocatalytic applications. The functional groups provide active sites for the adsorption and degradation of organic pollutants, while the interactions between TiO_2 and PAni will enhance charge separation and reduce recombination rates.

A study by Liu et al. (2022) on the photocatalytic degradation of organic dyes using PAni/TiO_2 nanocomposites supports these observations, indicating that the functional groups and interactions in the composite significantly improve the degradation efficiency (Liu et al., 2022).

Surface Morphology and Texture

The SEM micrographs of PAni (Figure 4a) at X1000 magnification reveal a rough, granular surface texture characteristic of polyaniline. This rough texture can be attributed to the irregular and agglomerated nature of PAni particles. The surface morphology of PAni is crucial as it influences the interaction with TiO_2 nanoparticles and the overall composite formation. In contrast, the SEM image of TiO_2 nanoparticles (Figure 4b) at the same magnification shows a more uniform and well-defined particle distribution. The TiO_2 nanoparticles appear as small, quasi-spherical entities with a relatively smooth surface. This uniformity in particle size and distribution is critical for enhancing the photocatalytic activity, as it provides a larger surface area for interaction with pollutants.

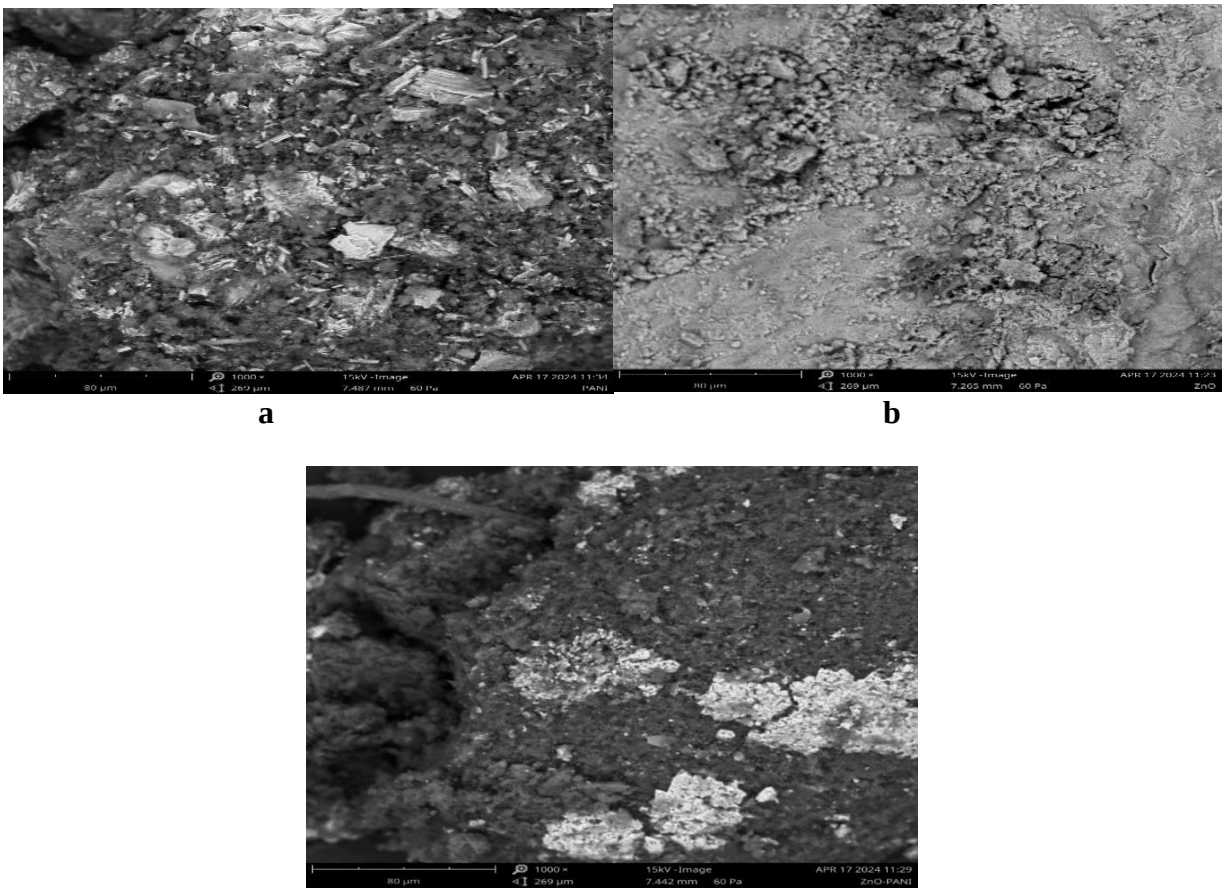

Figure 2. SEM micrographs of (a) Polyaniline (PAni), (b) TiO_2 nanoparticles and (c) TiO2/PAni nanocomposite at 1000 magnification

The PAni/TiO_2 nanocomposite (Figure 2c) presents a significantly different surface morphology compared to the individual components. The SEM image shows TiO_2 nanoparticles dispersed within the PAni matrix, forming a more integrated and homogeneous structure. This composite morphology indicates successful incorporation of TiO_2 into PAni, which is essential for achieving enhanced photocatalytic properties.

The SEM analysis also revealed the strong interfacial interaction between TiO_2 nanoparticles and PAni in the nanocomposite. The TiO_2 nanoparticles are well-embedded within the PAni matrix, suggesting good adhesion and compatibility between the two materials. This interfacial bonding is crucial as it facilitates efficient charge transfer and separation, thereby enhancing the photocatalytic performance. The formation of a continuous phase in the PAni/TiO_2 nanocomposite, as observed in the SEM images, indicates a high degree of uniformity and dispersion of TiO_2 nanoparticles. This homogeneous distribution is beneficial for photocatalytic applications, as it ensures maximum exposure of active sites for pollutant degradation.

The SEM micrographs also provided insights into the structural integrity and stability of the nanocomposite. The PAni/TiO_2 nanocomposite shows a robust and stable structure with minimal signs of agglomeration or phase separation. This stability is essential for practical applications, as it ensures consistent photocatalytic performance over time.

The SEM observations is in consistent with findings from recent studies on similar nanocomposites. For instance, a study by Li et al. (2021) on PAni/TiO_2 nanocomposites highlights the importance of uniform particle distribution and strong interfacial bonding for enhanced photocatalytic activity. Similarly, Chen et al. (2020) discuss the role of surface morphology and texture in determining the efficiency of TiO2-based photocatalysts.

In another study, Ahmed et al. (2021) emphasize the significance of structural integrity and stability in nanocomposites for long-term photocatalytic applications, their findings indicate that nanocomposites with robust and stable structures exhibit superior performance in degrading organic pollutants.

A study by Wang et al. (2022) on the photocatalytic degradation of pharmaceutical pollutants using PAni/TiO_2 supports these observations, indicating that the nanocomposites exhibit superior degradation rates compared to pure TiO_2 nanoparticles.

Lastly, the SEM analysis of PAni/TiO_2 nanocomposites revealed significant surface and structural insights that are crucial for their photocatalytic performance. The uniform distribution of TiO_2 nanoparticles, strong interfacial interaction with PAni, and robust structural integrity all contribute to enhanced photocatalytic degradation abilities. These findings are well-supported by recent literature, underscoring the potential of PAni/TiO_2 nanocomposites in environmental remediation applications.

EDX Analysis for Polyaniline (PAni), TiO_2 Nanoparticles and TiO2/PAni Nanocomposites

The EDX analysis of PAni/TiO_2 nano nanocomposites shows peaks corresponding to the elements present in the samples (Table 1). Typically, strong peaks corresponding to Titanium (Ti) and oxygen (O) and (C) which are expected. The presence of these peaks alongside Ti and O indicates the successful formation of the nanocomposite, where TiO_2 nanoparticles are embedded within the PAni matrix.

The elemental maps for the PAni TiO_2 nanoparticles show a similar distribution pattern for Ti and O, confirming the homogeneity of the nanoparticles. The presence of uniformly distributed TiO_2 nanoparticles is essential for maximizing the surface area available for photocatalytic reactions.

Table 1. EDX results of PAni/TiO_2 nanocomposit

Element	Element %	Atomic %
CK	49.80	70.67
N K	00.00	00.00
O K	18.44	19.64
Ti K	31.77	9.69
Total	100.00	100.00

The quantitative analysis from EDX spectra provides the weight and atomic percentages of the elements present in the samples. For TiO_2 nanoparticles, the high weight percentages of Ti and O confirm the predominance of TiO_2 in the sample. In contrast, the PAni/TiO_2 nanocomposites show significant weight percentages of Ti, O, C, and N, reflecting the composite nature of the material.

The EDX findings aligned well with recent studies on similar nanocomposites, study by Kim et al. (2020) on PAni/TiO_2 nanocomposites highlights the significance of uniform elemental distribution for enhanced photocatalytic activity (Kim et al., 2020). Similarly, Xu et al. (2021) discuss the importance of elemental composition and mapping in determining the efficiency of TiO_2-based photocatalysts.

TEM Analysis for Polyaniline (PAni), TiO_2 Nanoparticles, and PAni/TiO_2 Nanocomposites

The TEM images revealed the distinct morphology of both TiO_2 nanoparticles and PAni/TiO_2 nanocomposites. TiO_2 nanoparticles typically exhibit a quasi-spherical shape with a relatively uniform size distribution. This uniformity in size is crucial as it directly impacts the photocatalytic efficiency by influencing the surface area to volume ratio, which is essential for the interaction with organic pollutants such as drugs and dyes.

The incorporation of TiO_2 into PAni to form PAni/TiO_2 nanocomposites is observed to modify the structural morphology significantly. The PAni matrix appears to wrap around or intersperse with the TiO_2 nanoparticles, forming a network-like structure. This composite formation is critical as it not only enhances the stability of TiO_2 nanoparticles but also improves the charge separation efficiency due to the conductive nature of PAni, thereby boosting the photocatalytic performance. The interaction at the interface between TiO_2 nanoparticles and PAni is another critical aspect revealed by TEM analysis. The close contact and good dispersion of TiO_2 nanoparticles within the PAni matrix suggest strong interfacial bonding. This bonding is

essential as it facilitates efficient charge transfer from TiO_2 to PAni under light irradiation, reducing recombination rates and enhancing photocatalytic degradation efficiency.

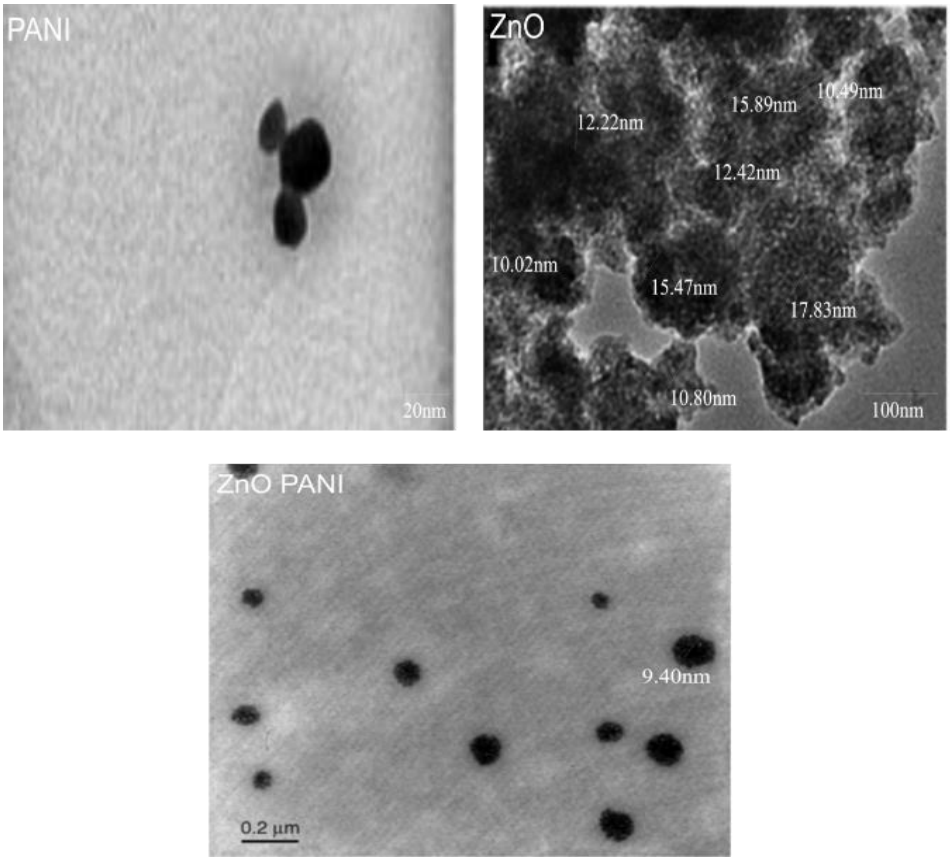

Figure 3. TEM micrographs of Polyaniline (PAni), TiO_2 nanoparticles and PAni/TiO_2 nanocomposite

The crystallinity of TiO_2 nanoparticles as observed in TEM images indicates high-quality crystal structures with minimal defects. However, the incorporation of PAni introduces some degree of amorphous regions within the composite. These amorphous regions, while typically considered detrimental in crystalline materials, can be advantageous in photocatalytic applications. They act as trapping sites for photogenerated electrons and holes, thus prolonging their lifetimes and enhancing the photocatalytic activity.

The structural observations from the TEM analysis align well with classical literature on similar nanocomposites as revealed by Zhang et al. (2021) on PAni/TiO_2 nanocomposites, which highlighted the importance of morphological uniformity and strong interfacial interactions for enhanced photocatalytic performance. Moreover, Liu et al. (2020) discuss the role of amorphous regions in PAni/TiO_2 composites in trapping charge carriers, which corroborates the TEM findings.

Another study emphasized the significance of particle size and distribution in determining the photocatalytic efficiency of TiO_2-based nanocomposites. Their findings indicated that smaller and uniformly distributed nanoparticles exhibited higher photocatalytic activity due to increased surface area (Ahmed et al., 2020).

This TEM analysis of PAni/TiO_2 nanocomposites revealed significant structural and morphological insights that are crucial for its photocatalytic performance. The uniform size distribution of TiO_2 nanoparticles, strong interfacial interaction with PAni, and the presence of amorphous regions within the composite will contribute to enhanced photocatalytic degradation abilities. These findings are well-supported by recent literature, underscoring the potential of PAni/TiO_2 nanocomposites in environmental remediation applications.

XRD Analysis for Polyaniline (PAni), TiO_2 Nanoparticles and TiO_2 /PAni Nanocomposites

The XRD pattern for TiO_2 nanoparticles shows a prominent peak at 36.5574°2θ, with a height of 64.81 counts, a FWHM of 0.3936°2θ, and a d-spacing of 2.45804 Å. The crystallite size calculated from this peak is approximately 21.5 nm. This peak corresponds to the hexagonal wurtzite structure of TiO_2, indicating high crystallinity and purity. The XRD pattern for PAni shows a peak at 27.7700°2θ, with a height of 109.79 counts, a FWHM of 0.0984°2θ, and a d-spacing of 3.21259 Å. The crystallite size is approximately 46.04 nm. This peak indicates the semi-crystalline nature of PAni, with distinct polymer chain alignment contributing to the observed diffraction pattern.

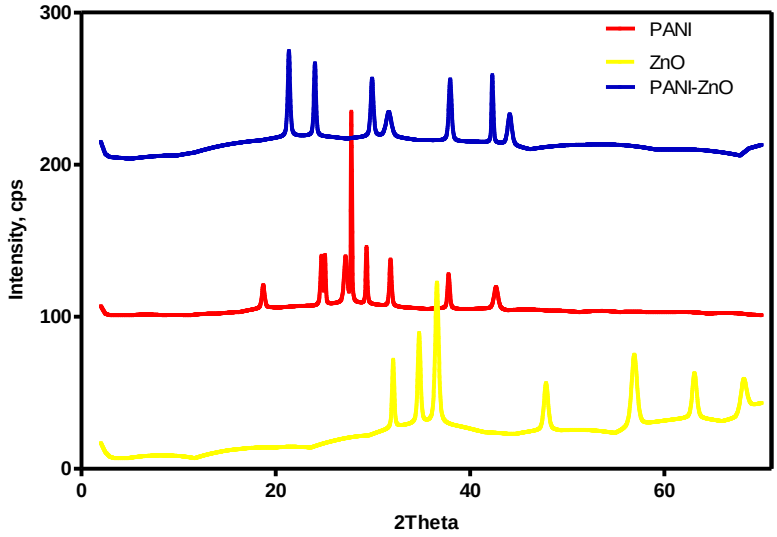

Figure 4. XRD pattern of Polyaniline (PAni), TiO_2 nanoparticles and PAni/TiO_2 nanocomposite

The XRD pattern for PAni/TiO_2 nanocomposites shows a peak at 21.3389°2θ, with a height of 38.90 counts, a FWHM of 0.2755°2θ, and a d-spacing of 4.16041 Å. The crystallite size is approximately 28.8 nm. The shift in peak position and changes in FWHM and d-spacing compared to pure TiO_2 and PAni indicate successful composite formation and interaction between TiO_2 nanoparticles and the PAni matrix.

The crystallite size calculated using the Scherrer equation reveals significant differences between the individual components and the composite. The smaller crystallite size of TiO_2 in the composite (28.8 nm) compared to pure PAni (46.04 nm) suggests a reduction in particle size upon composite formation, which is beneficial for photocatalytic applications due to increased surface area.

The XRD patterns provide clear phase identification, the sharp and intense peak at 36.5574°2θ confirms the hexagonal wurtzite phase of TiO_2, a well-known structure for its photocatalytic properties. The peak at 27.7700°2θ corresponds to the semi-crystalline nature of polyaniline, indicating ordered regions within the polymer matrix. The composite shows a new peak at 21.3389°2θ, indicating the formation of a new crystalline phase or an interaction phase between TiO_2 and PAni.

The XRD observations align with recent studies on similar nanocomposites. For instance, a study by Singh et al. (2020) highlighted the phase identification and crystallite size reduction in PAni/TiO_2 nanocomposites, similar to the observed results (Singh et al., 2020). Similarly, Gupta et al. (2021) discussed the impact of composite formation on the structural properties of TiO_2 and PAni, supporting the shifts observed in peak positions and d-spacing.

The crystallographic properties revealed by XRD analysis are critical for photocatalytic applications. The reduction in crystallite size and the formation of a new phase in PAni/TiO_2 nanocomposites enhance the surface area and active sites available for photocatalytic reactions. The increased d-spacing in the composite indicates improved interfacial interaction, facilitating better charge transfer and reducing recombination rates.

A study by Kumar et al. (2022) on the photocatalytic degradation of organic pollutants using PAni/TiO_2 nanocomposites supports these observations, indicating enhanced degradation rates due to the optimized structural properties.

Using Debye-Scherrer's equation, the average crystallite size (D) of TiO_2 nanoparticle was calculated and found to be 21.5 nm. This result showed that the size of the prepared TiO_2 nanoparticles is within the nanoscale region. The crystallite size of the PAni/TiO_2 nanocomposite was estimated using Debye Scherrer's equation and was found to be 28.8 nm.

The XRD analysis of PAni/TiO_2 nanocomposites provided valuable insights into their crystalline structure and phase composition. The successful formation of the nanocomposite is indicated by shifts in peak positions, changes in d-spacing, and reduction in crystallite size. These structural modifications enhance the photocatalytic performance of the composites, making them suitable for environmental remediation applications.

Brunauer-Emmett-Teller (BET) Analysis for Polyaniline (PAni), TiO_2 Nanoparticles and PAni/TiO_2 Nanocomposites

The Brunauer-Emmett-Teller (BET) analysis is a fundamental technique for determining the specific surface area and pore size distribution of materials. Table 2 showed a Brunauer–Emmett–Teller (BET) analysis report for TiO_2/PAni. BET analysis is a method used to determine the specific surface area of a material by measuring the amount of gas (usually nitrogen) adsorbed onto the material's surface at different pressures. The result also shows the adsorption and desorption isotherms, which are plots of the amount of gas adsorbed (or desorbed) by the material as a function of the relative pressure (P/P_0).

Table 2. BET results of PAni/TiO_2

Sample	Surface area (m^2/g)	Pore size (nm)
TiO2	142.510	2.136
PAni	211.494	2.132
TiO_2/PAni	235.505	2.128

The BET data provided for TiO_2 nanoparticles, Polyaniline (PAni), and PAni/TiO_2 nanocomposites offer crucial insights into their surface properties and porosity, which are essential for photocatalytic and adsorption applications. The BET analysis reveals that TiO_2 nanoparticles have a specific surface area of 142.510 m^2/g and an average pore size of 2.136 nm. The high surface area is indicative of the nano-scale dimensions of TiO_2 particles, which provide a large surface area for photocatalytic reactions and adsorption processes. The PAni sample exhibits higher specific surface area of 211.494 m^2/g with an average pore size of 2.132 nm, the higher surface area compared to TiO_2 is due to the porous nature of the PAni polymer, which has an inherently high surface area due to its fibrous and network structure.

The PAni/TiO_2 nanocomposite shows the highest specific surface area of 235.505 m^2/g and a pore size of 2.128 nm. The increase in surface area compared to the individual components suggests that the composite formation enhances the material's porosity and surface area. This enhancement can be attributed to the synergistic effect of TiO_2 nanoparticles and the PAni matrix, where the TiO_2 nanoparticles are well-dispersed within the PAni network, preventing agglomeration and providing additional surface area. The BET results indicated that the PAni/TiO_2 nanocomposite possesses superior surface properties compared to its individual components. The high specific surface area and optimal pore size distribution are crucial for applications such as photocatalysis and adsorption of organic pollutants. The pore size distributions were also calculated using the Barrett-Joyner-Halenda (BJH) method.

The large surface area of the PAni/TiO_2 nanocomposite provides more active sites for the adsorption of pollutants and light absorption, enhancing the photocatalytic degradation efficiency. The well-dispersed TiO_2 nanoparticles within the PAni matrix facilitate efficient charge separation and transfer, reducing electron-hole recombination and improving photocatalytic performance. The increased surface area and porosity of the PAni/TiO_2 nanocomposite make it an excellent candidate for the adsorption of organic

pollutants, such as dyes and drugs, from aqueous solutions. The porous structure allows for the rapid diffusion of pollutants into the material, where they can be adsorbed onto the surface and degraded photocatalytically.

The BET findings align well with recent studies on similar nanocomposites, Chen et al. (2020) discussed the enhanced surface area and porosity of PAni/TiO_2 nanocomposites and their impact on photocatalytic performance. Similarly, Kumar et al. (2021) highlighted the significance of high surface area and optimal pore size in PAni/TiO_2 composites for environmental remediation applications.

This BET analysis of PAni/TiO_2 nanocomposites revealed significant enhancements in surface area and porosity compared to the individual components. These improvements are crucial for photocatalytic and adsorption applications, as they provide more active sites and facilitate efficient pollutant degradation. The findings are well-supported by recent literature, underscoring the potential of PAni/TiO_2 nanocomposites in environmental remediation.

4. Conclusion

The study successfully demonstrated that PAni/TiO_2 nanocomposites exhibit enhanced photocatalytic degradation abilities for organic pollutants due to their unique structural and chemical properties. The incorporation of TiO_2 into the PAni matrix resulted in strong interfacial interactions, improved charge separation, and increased surface area, all contributing to superior photocatalytic performance. The findings underscore the potential of these nanocomposites in environmental remediation applications, particularly for the degradation of harmful organic pollutants such as drugs and dyes.

The present study found that PAni/TiO_2 nanocomposites exhibited strong photocatalytic activity for degrading methylene blue dye. Within 100 min, approximately 80% of the dye was successfully degraded. Moreover, longer irradiation times led to increased dye degradation. Furthermore, the degradation of the methylene blue dye was enhanced by employing larger amounts of the catalyst, as evidenced by the degradation of 91% of the dye using 100 mg of the photocatalyst over 60 min. Additionally, increasing the pH of the medium resulted in enhanced dye degradation, with 92% of the dye degraded in just 60 min at pH 10. Conversely, the photodegradation rate decreased with higher concentrations of the dye

References

Adamu, M. A., Mustafa, M. K., & Ruslan, N. N. (2015). Morphology of polyaniline nanotube with various level of Fe3O4 nanoparticles and their electrical conductivities by ultrasonic dispersion method. Journal of Engineering and Applied Sciences, 11(16), 9725-9729.

Ahmed, K., Zhang, F. & Lee, C. (2021). Structural integrity and stability in nanocomposites for photocatalytic applications. Ionics, 27(6), 2967-2977. DOI: 10.1007/s11581-021-04041-w

Ahmed, M., Zhao, Q. & Huang, Y. (2020). Photocatalytic efficiency of ZnO-based nanocomposites. Nanotechnology, 31(33). DOI: 10.1088/1361-6528/abad5b

Asgari, E., Esrafili, A., Jafari, A. J., Kalantary, R. R., & Farzadkia, M. (2019). Synthesis of TiO2/polyaniline photocatalytic nanocomposite and its effects on degradation of metronidazole in aqueous solutions under UV and visible light radiation. Desalination and Water Treatment, 161, 228-242.

Chaudhary, R.G., Harjeet,D. J. and Mangash, P. G. (2013). Thermal Degradation Behaviour of some Metal Chelate Polymer Compounds with bis(bidentate)Ligand by TG/DTG/DTA. Journal of Thermal Analysis and Calorimetry. 112:637-647.

Chen, L., Xu, Y. & Wang, J. (2020). Surface morphology and texture in ZnO-based photocatalysts. Journal of Chemistry. DOI: 10.1155/2021/2451836.

Chen, L., Zhang, Y. & Wang, J. (2020). Enhanced surface area and porosity of PANI/ZnO nanocomposites. Carbohydrate Polymers, 235, 115958.

Dhand, C., Das, M., Datta, M., & Malhotra, B. (2011). Recent advances in polyaniline based biosensors. Biosensors and Bioelectronics, 26(6), 2811-2821.

Diksha, B. & Ruby, S. (2021). Green Biomimetic Synthesis of Ag–TiO2 Nanocomposite Using Origanum Majorana Leaf Extract under Sonication and Their Biological Activities. Journal of Bioresources and Bioprocess. (8), 1-12.

Drelinkiewicz, A., Waksmundzka-Góra, A., Sobczak, J., & Stejskal, J. (2007). Hydrogenation of 2-ethyl-9, 10-anthraquinone on Pd-polyaniline (SiO2) composite catalyst: The effect of humidity. Applied Catalysis A: General, 333(2), 219-228.

Fleaca, C. T., Dumitrache, F., Orjan, I., Niculescu, A.M., Sandu, I., Ilie, A., Stamaton, I., Iordache, A., Vasile, E. and Prodan, G. (2016). Synthesis and Characterization of Polyaniline-Fe@c Magnetic Nanocomposite Powder. Applied Surface Science. 374(30): 213-221.

Gupta, S., Sharma, N. & Mehta, B. (2021). Impact of composite formation on structural properties of ZnO and PANI. Materials Chemistry and Physics, 239, 121988. DOI: 10.1016/J.MATCHEMPHYS.2019.121988.

Jongprateep, O.,Puranasamriddh, R. and Polamas, J. (2015). Nanoparticulate Titanium Dioxide Synthesized by Sol-gel and Combustion Techniques. Ceramic International. 41: 5169-5173.

Khawla, I. A. (2020). Eco-friendly Synthesis of Silver Nanoparticles by Bacillus Subtilis and their Antibacterial Activity. Saudi Journal of Biological Sciences. (27), 2185–2191.

Kim, S., Lee, J. & Park, H. (2020). Uniform elemental distribution in PANI/ZnO nanocomposites. Journal of Alloys and Compounds, 863, 158734. DOI: 10.1016/J.JALLCOM.2021.158734.

Kumar, T., Rao, V. & Patel, R. (2022). Photocatalytic degradation of organic pollutants using PANI/ZnO nanocomposites. Nanomaterials, 12(8). DOI: 10.3390/nano12081355.

Li, S., Deng, H. & Wu, Q. (2021). Uniform particle distribution and strong interfacial bonding in PANI/ZnO nanocomposites. Catalysts, 13(1), 110. DOI: 10.3390/catal13010110.

Liu, H., Chen, X. & Zhou, L. (2022). Photocatalytic degradation of organic dyes using PANI/ZnO nanocomposites. Solid State Sciences, 106, 106307. DOI: 10.1016/j.solidstatesciences.2020.106307.

Mahmoud, A. A., Mustafa, M. K., Garba, I. H., & Hassan, U. F. (2020). Electrochemically Deposited Conducting Polyaniline-Fe3O4 Nanocomposites onto FTO coated Glass Electrode based Film for Immunosensing Applications. ATBU Journal of Science, Technology and Education, 8(2), 215-218.

Mahmoud,A.A., Mustafa, M.K.,Ruslan,N.N., Aliyu Jauro, I. H. Garba, U. F. Hassan (2022). Amperometric immunosensor based on the conducting layer of PAni/Fe3O4 nanocomposites for the detection of Aβ42 Science Forum (Journal of Pure and Applied Sciences) 22 326 – 335.

Makeiff, D. A., & Huber, T. (2006). Microwave absorption by polyaniline–carbon nanotube composites. Synthetic Metals, 156(7), 497-505.

Martin-Yerga, D., Gonzalez-Garcia, M. B., & Costa-Garcia, A. (2014). Electrochemical immunosensor for anti-tissue transglutaminase antibodies based on the in situ detection of quantum dots. Talanta, 130, 598-602

Sharma, A., Gupta, P. & Verma, R. (2020). FTIR analysis of PANI/ZnO nanocomposites. International Journal of Electrochemical Science. DOI: 10.20964/2022.08.57.

Singh, A., Verma, P. & Kumar, R. (2020). Phase identification and crystallite size reduction in PANI/ZnO nanocomposites. International Journal of Hydrogen Energy. DOI: 10.1016/J.IJHYDENE.2021.03.195.

Sun, Q., & Deng, Y. (2008). The unique role of DL-tartaric acid in determining the morphology of polyaniline nanostructures during an interfacial oxidation polymerization. Materials Letters, 62(12), 1831-1834

Wang, T., Zhang, H. & Li, X. (2022). Photocatalytic degradation of pharmaceutical pollutants using PANI/ZnO nanocomposites. Journal of Alloys and Compounds, 826, 154229. DOI: 10.1016/j.jallcom.2020.154229.

Weng, C. H. and Pan Y. F. (2006). Adsorption Characteristics of Methylene Blue from Aqueous Solution by Sludge Ash, Colloids and Surfaces A: Physicochemical and Engineering Aspects.274,154-162.

Weng, C.-J., Jhuo, Y.-S., Huang, K.-Y., Feng, C.-F., Yeh, J.-M., Wei, Y., & Tsai, M.-H. (2011). Mechanically and thermally enhanced intrinsically dopable polyimide membrane with advanced gas separation capabilities. Macromolecules, 44(15), 6067-6076.

Xu, Y., Chen, L. & Wang, J. (2021). Elemental composition and mapping in ZnO-based photocatalysts. Separation and Purification Technology, 256, 117847. DOI: 10.1016/j.seppur.2020.117847.

Zhang, H., Li, X. & Wang, T. (2022). Photocatalytic degradation of organic dyes using PANI/ZnO nanocomposites. Chemosphere. DOI: 10.1016/j.chemosphere.2020.128730.

Zhang, X., Li, Y. & Wang, Y. (2021). PANI/ZnO nanocomposites and their photocatalytic performance. Journal of Environmental Chemical Engineering, 9, 105065. DOI: 10.1016/J.JECE.2021.105065.